

THE CRYSTAL STRUCTURE AND GENESIS OF KRENNERITE, Au_3AgTe_8

MATTHEW D. DYE[§] AND JOSEPH R. SMYTH[‡]

Department of Geological Sciences, University of Colorado, Boulder, Colorado 80309-0399, U.S.A.

ABSTRACT

The crystal structure of a natural krennerite (Au_3AgTe_8) from Cripple Creek, Colorado, USA has been refined in space group *Pma2* using 3,151 observed unique (acentric) reflections. The final *R* value for observed reflections was 0.022. Unit cell parameters are *a* 16.590(3) Å, *b* 8.867(2) Å, *c* 4.4886(8) Å, *V* 660.29(13) Å³, and *Z* = 2. The precision of the atom position parameters is improved by up to a factor of ten over previous studies. The three Au–Ag sites in the structure are ordered, with Ag = 43% occupancy at the Au1 (2*a*) position (point symmetry 2) and 59% at the Au2 (2*c*) position (point symmetry *m*); the Au3 (4*d*) position (point symmetry 1) is 100% Au. The observed ordering in the structure appears to be due to avoidance of Ag–Te–Ag bonding. Ordering of Au and Ag in the structure may thus limit the composition range to being between those of calaverite and sylvanite. Detailed petrographic study of the sample in thin section, accompanied by electron microprobe data, demonstrates the paragenesis of the ore that provided the crystal for refinement. The petrographic study provides evidence for sylvanite exsolution from krennerite in natural systems, consistent with the narrow compositional range inferred from the crystallographic study.

Keywords: krennerite, crystal structure, Au–Ag telluride minerals, paragenesis, exsolution, Cripple Creek

INTRODUCTION

One of the very few chemical elements with which Au forms stoichiometric solids in nature is Te, which happens to be one of the least abundant elements in the Earth's crust. Therefore, examination of the details of the crystal chemistry of Au telluride minerals may shed some light on the geochemistry of Au and Te, both economically important rare elements. Krennerite is one of three primary Au–Ag telluride minerals: calaverite, krennerite, and sylvanite. These telluride minerals have the general formula $(\text{Au},\text{Ag})\text{Te}_2$, but are distinguished both by crystal structure and by specific levels of Ag substitution. Based on synthesis studies, calaverite has a compositional range of 0.0 to 2.8 wt.% Ag, krennerite 3.4 to 6.2 wt.% Ag, and sylvanite 6.7 to 13.23 wt.% Ag (Cabri 1965). Although the krennerite species is relatively rare, it is known from numerous localities including the Cripple Creek, Boulder County, and La Plata mining districts of Colorado, USA, along with scattered occurrences in Arizona, California, and Montana (Geller 1993). Globally, important krennerite localities include the Baia de Aries (Offenbánya) and Nagyág (Sacarimb) regions of Romania, the Emperor Mine in Vatukoula, Fiji, and the Goldfields–Esperance Region in Kalgoorlie, Australia (Cabri 1965, Geller 1993).

BACKGROUND INFORMATION

Whereas calaverite and sylvanite share similar centric monoclinic structures, the chemically intermediate krennerite is acentric and orthorhombic. The crystal structures of the three Au–Ag tellurides are closely related, with each having the noble metal atoms in distorted octahedral coordination with Te. Calaverite (AuTe_2) is monoclinic with four Te atoms per cell, sylvanite (AuAgTe_4) is monoclinic with eight Te per cell, and krennerite is acentric orthorhombic with 16 Te per cell (Pertlik 1984a,b). Both calaverite and sylvanite show complex incommensurate super-lattice ordering structures (Schutte and deBoer 1988), whereas krennerite does not. The structure of krennerite was originally determined by Tunell & Ksanda (1936) and refined by Tunell & Murata (1950) in space group *Pma2*. The structure was further refined by Pertlik (1984b), who noted the ordering of the Au and Ag atoms among the three distinct octahedral sites. The octahedra form zigzag sheets that are connected only by common Te–Te bonds (Fig. 1). The unit cell of krennerite consists of 16 Te atoms in five crystallographically distinct sites and eight Au/Ag atoms ordered in three distinct sites. Two of the Au/Ag sites, Au1 and Au2, are special (two per cell), and one, Au3, is general (four per cell). The Ag atoms appear to be restricted to the special positions (Pertlik 1984b).

[§] E-mail address: mdye@mymail.mines.edu [‡] smyth@colorado.edu

Recent advances in X-ray CCD instrumentation and high intensity X-ray sources have made it practical to measure large intensity data sets from very small crystals (<40 μm) that allow for much greater precision in atom position parameter and occupancy refinement. In order to measure Au-Ag ordering in the Cripple Creek sample and understand the role of ordering on composition ranges, we have undertaken the refinement of the krennerite structure.

EXPERIMENTAL

Samples

The specimen used in this study was part of the mineralogy collection at the University of Colorado Museum, UCM No. 1641. It was collected at the Little Clara Mine in the Cripple Creek District, Colorado by University Regent H.D. Thompson sometime around the year 1900. This mine was part of the Doctor-Jackpot claim block, which lies 1.2 km to the west-northwest of the Cresson Mine. The specimen consists of bladed, subhedral crystals of sylvanite and krennerite up to 1.5 mm in length on a substrate of matrix-supported volcanoclastic material, generally referred to as the "Cripple Creek Breccia". The sample itself was incorrectly labeled as calaverite, and was only found to contain krennerite after obtaining an initial X-ray diffraction pattern from a single crystal removed from the face of the specimen.

X-ray Diffraction

X-ray diffraction work was conducted using an automated four-circle goniometer equipped with a Bruker APEX II CCD detector for intensity data. Unit cell parameter refinements were made using a Bruker P4 point detector diffractometer. The X-ray source for both the point detector and the CCD detector was a Bruker rotating molybdenum anode X-ray generator operating at 50 KV and 250 mA.

A cleavage fragment from a single crystal taken from the Little Clara Mine sample, measuring about $25 \times 25 \times 6 \mu\text{m}$, was attached to a glass filament and mounted on the automated four-circle goniometer. An initial scan of 72 ten-second exposure frames was conducted, and indexing on the krennerite cell confirmed the identification. A series of chi and omega scans covering a full sphere of reciprocal space was then performed to a two-theta maximum of 75° . This led to a final *hkl* output file consisting of 18,882 reflections. Of these, 467 had intensities of less than 3σ based on counting statistics, and were rejected. Of the remaining 18,415 returned reflections, 3,407 were unique, and 3,151 of the unique reflections had intensities greater than 4σ . Equivalent reflection intensities were averaged, but Friedel pairs were not averaged. No explicit absorption correction was performed as an entire sphere of

intensity data was measured and equivalents averaged. The unit cell parameters were refined using a Bruker P4 point detector diffractometer to give $a = 16.590(3) \text{ \AA}$, $b = 8.867(2) \text{ \AA}$, and $c = 4.4886(8) \text{ \AA}$.

Atom parameters of Pertlik (1984b) were then refined using SHELXL (Sheldrick 1997). The structure refined to an $R(F)$ of 0.11 using isotropic displacement parameters. Initial refinements gave a Flack X parameter of 1.0, though it should be near zero for the correct enantiomorph (Flack 1983). We then inverted the position parameters and set the Au1 z -parameter to zero to define the cell origin at a more convenient location. Using anisotropic displacement parameters, the final refinement converged to an $R(F)$ of 0.024 for the 3,151 unique reflections and 0.022 for the 1,932 unique reflections after merging Friedel pairs. The resulting structure of krennerite is shown as an ellipsoidal model in Figure 2. Occupancies of the Au sites were modeled using neutral-atom scattering factors for Ag, Au, and Te. Occupancy refinements of these sites show that the structure is ordered with the Au1 position containing 43% Ag (atomic) and 57% Au, the Au2 position containing 59% Ag and 41% Au, and the Au3 position 100% Au. Occupancy refinements, assuming full occupancy of the three Au-Ag sites, are consistent with the electron microprobe chemical analysis discussed in the next section.

Final atomic position, anisotropic displacement, and occupancy parameters are given in Table 1. Table 2 lists selected inter-atomic distances with relevant coordination polyhedron geometric parameters, and Table 3 gives the principle mean square atomic displacements for each atom. The largest positive residual in the differ-

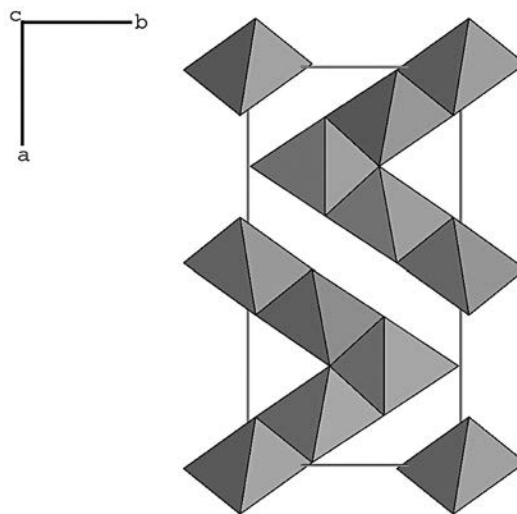


Fig. 1. The polyhedral structure of krennerite parallel to [001].

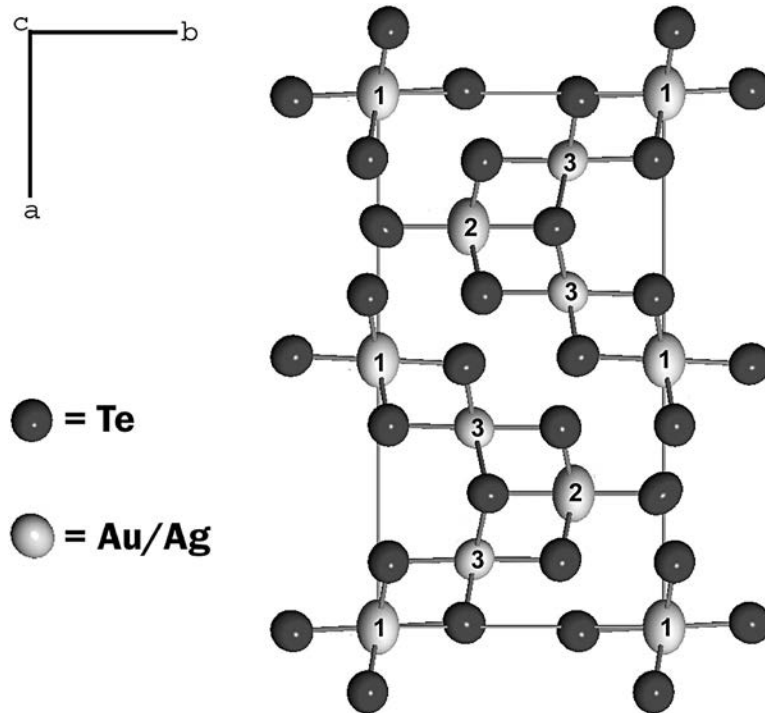


Fig. 2. Ellipsoidal model of krennerite sample 1641 perpendicular to [001]. Au-site numbers are labeled for reference.

TABLE 1. FRACTIONAL COORDINATES, OCCUPANCY, AND DISPLACEMENT PARAMETERS FOR KRENNERITE 1641

Atom	x/a	y/b	z/c	Occ.*	U_{11}	U_{22}	U_{33}	U_{23}	U_{13}	U_{12}
Au1	0	0	0	0.574(2) Au 0.426(2) Ag	0.0208(2)	0.0124(2)	0.0228(2)	0	0	0.0015(1)
Au2	0.75	0.68359(4)	0.99888(15)	0.413(2) Au 0.587(2) Ag	0.0224(2)	0.0121(2)	0.0312(2)	-0.0002(2)	0	0
Au3	0.87326(1)	0.33624(2)	0.51017(13)	0.997(2) Au	0.0119(1)	0.0111(1)	0.0171(1)	-0.0010(1)	-0.0025(1)	0.0003(1)
Te1	0.75	0.98757(5)	0.05372(16)	1 Te	0.0129(2)	0.0133(2)	0.0166(2)	-0.0026(2)	0	0
Te2	0.75	0.38423(5)	0.13089(16)	1 Te	0.0107(2)	0.0120(2)	0.0154(2)	0.0005(2)	0	0
Te3	0.99237(2)	0.30122(3)	0.91171(17)	1 Te	0.0120(1)	0.0124(1)	0.0150(1)	0.0007(1)	-0.0007(1)	-0.0005(1)
Te4	0.87443(2)	0.63750(4)	0.53488(15)	1 Te	0.0131(1)	0.0118(1)	0.0175(2)	-0.0005(1)	0.0006(1)	-0.0005(1)
Te5	0.87800(2)	0.03659(4)	0.46685(15)	1 Te	0.0127(1)	0.0115(1)	0.0173(2)	-0.0002(1)	0.0010(1)	-0.0002(1)

ence Fourier was at (0.25, 0.978, 0.197), very close to the Te1 position at the apex of the zigzag sheets, and might represent slight positional disorder in this atom, or possibly electrons involved in Te-Te bonding as discussed below.

Electron microprobe

Electron microprobe work was conducted using a JOEL JXA-8600 Superprobe at the University of Colorado. All analyses were performed using wavelength-

dispersive spectroscopy (WDS) with standards for both Au and Ag. Tellurium content was determined using the difference method. Secondary energy dispersive spectroscopy (EDS) was also utilized in each analysis to ensure the Te values returned by WDS did not include evidence of other chalcophile metals, such as Pb or Cu.

Three polished sections were made using material cut from sample 1641. In agreement with previous visual identifications, sylvanite was shown to be the most abundant telluride phase present in the polished sections, with krennerite representing the second most

abundant telluride phase. The approximate ratio of optically observed sylvanite grains to optically observed krennerite grains was 5:1. A total of 20 krennerite grains were analyzed in order to determine their Ag content. In these analyses, Ag content ranged from 4.71-6.05 wt.%, averaging 5.59 wt.%. A total of 19 sylvanite grains were also analyzed for the purpose of comparison, showing a Ag range of 7.17-9.49 wt.%. The average Ag content of the sylvanite was 8.89 wt.%. Microprobe analyses for krennerite are summarized in Table 4 and are consistent with that derived from X-ray diffraction. The average empirical formula for krennerite is shown to

be $Au_{2.9}Ag_{0.9}Te_8$. Microprobe data for sylvanite shows the average empirical formula to be $Au_{1.3}Ag_{0.6}Te_4$. The analyses show no compositional overlap between krennerite and sylvanite.

DISCUSSION

Crystal Structure

The structure reported here is essentially the same as that of Pertlik (1984b), except for the inversion of the absolute structure and a minor displacement of the arbitrary origin in the *c*-direction. It is possible that both enantiomorphs are present in nature, but our crystal was small enough that only one was present in the sample. It remains unknown whether depositional conditions favor one enantiomorph over the other. Despite the similarity of the reported structures, our refinement yielded a six to ten-fold increase in the precision of the atom coordinates relative to the structure derived by Pertlik (1984b). The improved resolution allows examination and visualization of details of the structure.

All Ag and Au atoms are in distorted octahedral coordination with Te (Table 2) and there are no short Au-Au distances in the structure. The Au1 site at the origin has point symmetry 2 and is occupied by 43% Ag and 57% Au. It is coordinated by two Te3 atoms at

TABLE 2. SELECTED INTER-ATOMIC DISTANCES AND COORDINATION PARAMETERS IN KRENNERITE

Au1 Octahedron	57% Au; 43% Ag	Au2 Octahedron	41% Au; 59% Ag
Au1-Te3(2)	2.7031(7) (Å)	Au2-Te1	2.7066(9) (Å)
Au1-Te5(2)	2.9314(6) (Å)	Au2-Te2	2.7197(8) (Å)
Au1-Te5(2)	3.1510(7) (Å)	Au2-Te4(2)	2.9607(8) (Å)
		Au2-Te4(2)	3.1963(8) (Å)
<Au1-Te>	2.9285(5) (Å)	<Au2-Te>	2.9568(5) (Å)
Polyhedral Vol	32.11 (Å ³)	Polyhedral Vol	33.05 (Å ³)
Oct. Ang. Var.	85.98	Oct. Ang. Var.	88.83
Quad. Elong.	1.032	Quad. Elong.	1.033
Au3 Octahedron	100% Au	Te-Te distances	
Au3-Te2	2.6946(5) (Å)	Te1-Te5 (2)	2.8525(7) (Å)
Au3-Te2	3.4821(4) (Å)	Te3-Te4	2.8353(7) (Å)
Au3-Te3	2.6926(6) (Å)		
Au3-Te3	3.3492(5) (Å)		
Au3-Te4	2.6737(7) (Å)		
Au3-Te5	2.6652(7) (Å)		
<Au3-Te>	2.9262(5) (Å)		
Polyhedral Vol	31.99 (Å ³)		
Oct. Ang. Var.	52.22		
Quad. Elong.	1.044		

TABLE 3. PRINCIPLE MEAN SQUARE ATOMIC DISPLACEMENTS (Å)

Au1	0.0228	0.0211	0.0121
Au2	0.0312	0.0224	0.0121
Au3	0.0183	0.0110	0.0108
Te1	0.0180	0.0129	0.0119
Te2	0.0154	0.0119	0.0107
Te3	0.0154	0.0124	0.0117
Te4	0.0177	0.0132	0.0116
Te5	0.0175	0.0125	0.0115

TABLE 4. SELECTED ELECTRON MICROPROBE CHEMICAL ANALYSES FOR KRENNERITE IN SAMPLE 1641

Analysis Point Weight Percent	1	2	3	4	5	6	Avg
Au	34.29	33.79	34.32	33.62	33.10	33.46	33.76
Ag	5.43	5.46	5.58	5.60	5.87	6.03	5.66
Te	60.29	60.76	60.10	60.78	61.03	60.52	60.58
Total	100.01	100.01	100.00	100.00	100.00	100.01	100.01
Atom Ratios							
Te	8.00	8.00	8.00	8.00	8.00	8.00	8.00
Au	2.95	2.88	2.96	2.97	2.91	2.87	2.92
Ag	0.85	0.85	0.88	0.87	0.91	0.94	0.88

2.70 Å, two Te5 atoms at 2.93 Å, and two Te5 atoms at about 3.15 Å (2 + 2 + 2 coordination). The Au2 site has point symmetry 2 and is occupied by 41% Au and 59% Ag. It is coordinated by Te1 at 2.71 Å, Te2 at 2.72 Å, two Te4 atoms at 2.96 Å, and two more Te4 at 3.20 Å (2 + 2 + 2 coordination). Au3 is at a general position (point symmetry 1) and is essentially 100% Au based on occupancy refinement. It is coordinated by Te2 at 2.69 Å, Te3 at 2.69 Å, Te4 at 2.67 Å, Te5 at 2.67 Å, Te3 at 3.35 Å, and a Te2 at 3.48 Å (4 + 2 coordination). The structure thus consists of crenulated sheets of octahedra that are separate and not connected by Au–Te bonds (Fig. 1).

The coordination of the Te atoms is considerably more irregular. There are five distinct Te sites in the structure. Atoms Te1 and Te2 have point symmetry 2, and the rest are at general positions (point symmetry 1). Atom Te1 is bonded to Au2 at 2.71 Å and two Te5 atoms at 2.85 Å. Atom Te2 is bonded only to Au; one Au2 at 2.72 Å and two Au3 atoms at 2.69 and 3.48 Å, respectively. Atom Te3 is bonded to one Au1 at 2.70 Å, one Au3 at 2.69 Å, and one Te4 at 2.84 Å. Atom Te4 is bonded to Au2 at 2.96 Å, Au3 at 2.67 Å, and to Te3 at 2.84 Å. Atom Te5 is bonded to Au1 at 2.93 Å, Au3 at 2.67 Å, and Te1 at 2.85 Å. In addition to the Au–Te bonds listed above, there are two short Te–Te distances that are not octahedral edges, Te1 to Te5 at 2.85 Å and Te3 to Te4 at 2.84 Å. These short Te–Te distances indicate that the structure is not ionic, precluding discussion of valence states. These short distances span the gap between the crenulated sheets, such that the sheets appear to be held together by Te–Te bonds. In addition, the largest electron-density residual peak (1.75 e⁻) in the refinement is at (0.25, 0.978, 0.197), which lies close to Te1 along the short Te1–Te5 distances and may thus represent electrons involved in Te–Te bonding that hold the sheets together.

Interestingly, there are no Te atoms bonded to both Au1 and Au2, the two sites that contain Ag. So, what is it about the structure that gives rise to the peculiar ordering of Ag at the Au1 and Au2 sites, and might this be related to the limited composition range of krennerite? There is no significant size difference between the sites that contain Ag (Au1 and Au2) and those that contain only Au (Au3) (Table 2). We propose the formula for krennerite as Au₃AgTe₈ because there are 16 Te atoms in the unit cell with Z = 2. This formula, therefore, shows the apparent integer ratio between Au and Ag to be 3:1. The persistence of this ratio is demonstrated in the empirical atomic ratios derived in our microprobe analyses (Table 4). One possibility that could account for the order and the stabilization of the orthorhombic structure at a three to one Au to Ag ratio is that it avoids Ag–Te–Ag bonds. This would imply a Ag avoidance principle analogous to the aluminum avoidance principle in framework silicates. A comparison of the crystallographic parameters derived in this study is summarized in Table 5. A major conclusion of the

structure study is that ordering of Au and Ag at about the three to one ratio is an essential part of the acentric orthorhombic structure that restricts the composition range of krennerite. This inference can then be used to clarify the paragenesis.

Paragenesis

An approximate paragenetic sequence was constructed for specimen 1641 in order to validate the textural relationships between krennerite and sylvanite, as observed both visually, using a reflected light polarizing microscope, and qualitatively, using the electron microprobe's backscattered electron imaging function. A polished thin section was prepared to evaluate the relationships between the gangue and ore minerals. The resulting paragenetic sequence (Fig. 3) provides a context regarding the depositional environment of the krennerite used in the crystal-structure refinement outlined above. Ore formation was characterized by early wall-rock alteration and gangue mineralization, followed by a period of sulfide deposition, and ending with telluride formation. Wall-rock alteration consisted of the replacement of mafic minerals by pyrite, and mild to moderate sericite (white mica) replacement of lithic feldspar grains. Titanium appears to have been mobilized during alteration, allowing for the deposition of rutile ± anatase during the early stages of gangue mineral formation.

Sulfide mineral precipitation began with early, coarse, euhedral pyrite. This was followed by the slightly later deposition of two different forms of tetrahedrite. The first is an idealized form of tetrahedrite, in the sense that it does not contain any appreciable As. We refer to this form as "ideal tetrahedrite", with the approximate formula of Cu₁₂Sb₄S₁₃. The second, paragenetically later, form is an arsenian intermediary between tetrahedrite and tennantite. EDS measurements showed the second form to contain more Sb than As, so

TABLE 5. COMPARISON OF CRYSTALLOGRAPHIC PARAMETERS FROM DIFFERENT STUDIES OF KRENNERITE

	Tunell & Murata (1950)	Pertlik (1984b)	This Work
a (Å)	16.54(3)	16.58(1)	16.590(3)
b (Å)	8.82(3)	8.849(5)	8.867(2)
c (Å)	4.46(3)	4.464(3)	4.4886(8)
Volume (Å ³)	650.6	654.942	660.289
Density (g/cm ³)	8.86	n/a	8.649
Z	2	2	2
Space Group	<i>Pma2</i>	<i>Pma2</i>	<i>Pma2</i>
# of Unique Reflections	n/a	1063	3151
Minimum Intensity	n/a	2σ	3σ
R value	n/a	5.80%	2.20%
Au wt. %	35.1	35.3	33.47
Ag wt. %	5.4	5.0	5.59

we refer to this form as “arsenian tetrahedrite” with the approximate formula $\text{Cu}_{12}(\text{Sb,As})_4\text{S}_{13}$. Ideal tetrahedrite was observed as 2–5 μm corroded grains, suggesting partial resorption during the subsequent formation of arsenian tetrahedrite. The activity of Fe appears to have decreased as sulfide deposition progressed. This is evidenced by the crystal chemistry of the two tetrahedrite minerals, both of which lack any discernable Fe content when analyzed using the electron microprobe.

Sulfide and sulfosalt precipitation were then followed by the deposition of Au–Ag telluride minerals. Textural relationships suggest that the available Ag content within the mineralizing fluids increased with time, as evidenced by the progressive increase of Ag-rich telluride species present in the sequence. This relationship is demonstrated in Figures 4 and 5, which show anhedral grains of krennerite surrounded by paragenetically later, optically continuous grains of sylvanite. This trend of early sulfide deposition followed by late telluride deposition is consistent with the proposed paragenetic sequence in the Cripple Creek district as described by Lovering & Goddard (1950) and Saunders (1986). The relative path of telluride mineralization through time, as observed in sample 1641, is shown in Figure 6. This path is superimposed upon a modified version of the phase diagram for the Au–Ag telluride minerals as originally developed by Cabri (1965).

No fluid-inclusion studies were performed during the course of the current research; thus there are no defi-

nite constraints on the temperature of telluride formation. Fluid-inclusion data derived by Saunders (1986) using material from the Cresson mine in Cripple Creek indicate a clustering of telluride-stage homogenization temperatures ranging from 150 to 175 °C. However, this temperature range did not include any pressure corrections because of uncertainties regarding the depth of formation, as well as the dominance of either hydrostatic or lithostatic pressure (Saunders 1986). If a minimum pressure correction of 30 °C is added to the temperature range described above, then the actual temperature range of telluride formation at the Cresson mine would be 180 to 205 °C.

The Little Clara mine lies just over 1 km from the western edge of the Cresson mine. We assume that the mineralizing fluids responsible for telluride deposition within specimen 1641 from the Little Clara Mine were approximately the same temperature as the mineralizing fluids at the Cresson Mine. The corrected temperature range of 180 to 205 °C was therefore used to set the slope of the path of mineralization through time in Figure 6. The endpoints of the path shown were inferred using the microprobe results described previously.

It is important to note that the path of mineralization changes from krennerite-stable to sylvanite-stable with increasing Ag content of the ore-forming fluids. During the transition from krennerite to sylvanite deposition, the mineralizing fluids pass through a broad miscibility gap in which both krennerite and sylvanite are ther-

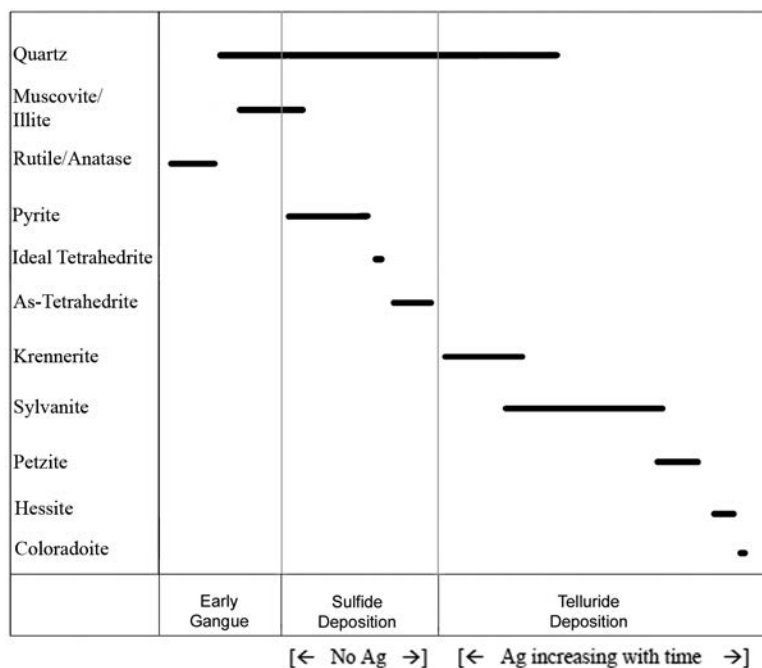


FIG. 3. Inferred paragenetic sequence of sample 1641.

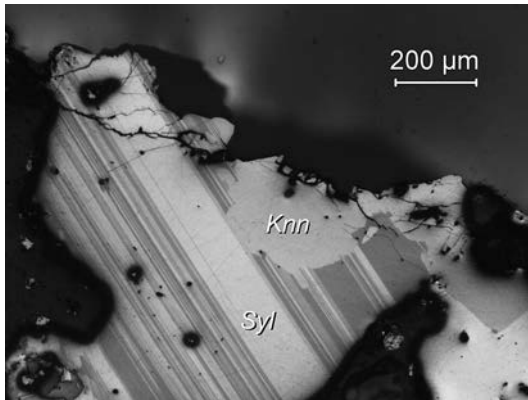


FIG. 4. Krennerite (Knn) grain enclosed by optically continuous sylvanite (Syl). Note the partial fragmentation of the krennerite grain prior to sylvanite mineralization. Crossed polars, 50× magnification.

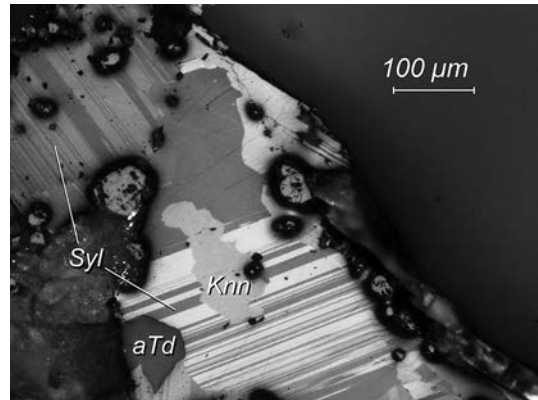


FIG. 5. Krennerite grain enclosed by optically continuous sylvanite. Note the association with arsenian tetrahedrite (aTd). Crossed polars, 100× magnification.

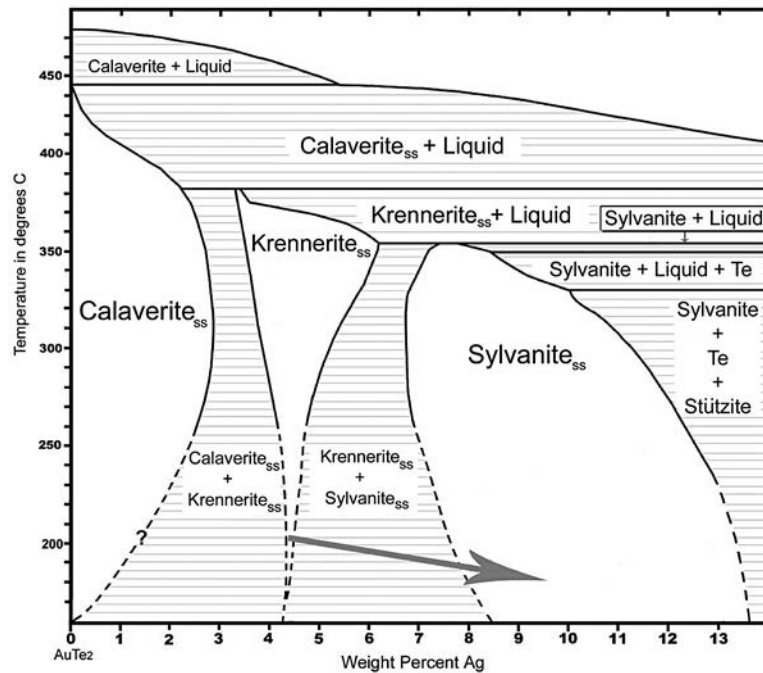


FIG. 6. Path of telluride mineralization through time at the Little Clara Mine. Tie lines between coexisting mineral phases shown in gray. Modified after L.J. Cabri 1965.

modynamically stable. This miscibility gap becomes wider with decreasing temperature and is important in explaining the possible exsolution of sylvanite from krennerite, as discussed below.

In the final stages of ore formation, sylvanite deposition appears to have caused the mineralizing fluids to become progressively depleted in Au, leading to the deposition of the Ag-rich telluride species petzite

(AuAg_3Te_4) and hessite (Ag_2Te). Paragenetically, the petzite appears to have preferentially formed at the perimeter of large sylvanite crystals and was also observed in contact with smaller crystals of both sylvanite and arsenian tetrahedrite. The petzite appears to have filled the last remaining free space within the quartz-lined cavities that host the krennerite and sylvanite crystals. Where in contact with one another, sylvanite and petzite share a common grain-boundary. This is interpreted to mean that petzite began to form as the result of a continued drop in available Au content with time, which would have rendered further sylvanite crystallization unstable. Note that petzite is not included in the phase diagram shown in Figure 6, although it has been proposed that sylvanite and petzite may form contemporaneously under specific conditions of low temperature (Cabri 1965).

Exsolution and Paragenesis

During the development of the paragenetic sequence, a single grain of krennerite was observed to contain what appeared to be exsolution lamellae. The lamellae are aligned parallel to one another within an otherwise homogeneous grain of krennerite (Figs. 7 and 8). In order to establish the chemical composition of these lamellae, several points were analyzed with the electron microprobe. The krennerite grain was also analyzed at two locations to verify its visual identification. The lamellae returned Ag contents of 7.17 to 7.71 wt.%, well within the range expected for sylvanite. The enclosing grain returned a value of 5.81 wt.% Ag, consistent with krennerite. Secondary EDS was again utilized to ensure that non-stoichiometric elements were not included in the returned values. To the best of the authors' knowledge, sylvanite exsolution from krennerite has not been

previously reported. However, the morphology of the lamellae seen here is indeed suggestive of exsolution. It is also possible that sylvanite replaced portions of a previously existing krennerite grain through the diffusion of Ag, but if so, one would expect irregular grain shapes rather than the observed lamellar texture. Furthermore, the miscibility gap between krennerite and sylvanite would seem to allow for the exsolution of sylvanite from krennerite, and vice versa (Louis J. Cabri, pers. commun.). A final piece of evidence for the plausibility of exsolution comes from the structures of krennerite and sylvanite themselves. The two structures are similar in the coordination and arrangement of the Au and Ag atoms, despite their differences in crystal system and space group.

The presence of exsolution lamellae implies that the two species coexisted and that the composition ranges became more restrictive on cooling (Fig. 6), as is commonly observed in many mineral systems, such as the pyroxenes and feldspars. It is unlikely that the exsolved mineral will ever represent anything more than a minor phase, which may be why there are few, if any, previously validated reports of krennerite-sylvanite exsolution in the literature. We do not know if exsolution is possible between calaverite and krennerite, but it seems less likely owing to the more significant structural differences between the two species.

SUMMARY

This study has revealed several details regarding the structure of natural krennerite. Perhaps the most noteworthy finding of this study is that Ag appears to be an essential component of the krennerite structure. The results of our single crystal X-ray diffraction analysis

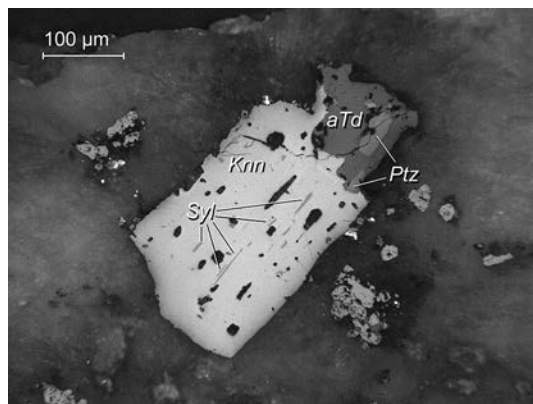


FIG. 7. Aligned exsolution (?) lamellae of sylvanite (Syl) within a grain of krennerite (Knn). Note the association with arsenian tetrahedrite (aTd) and petzite (Ptz). Crossed polars, 100 \times magnification.

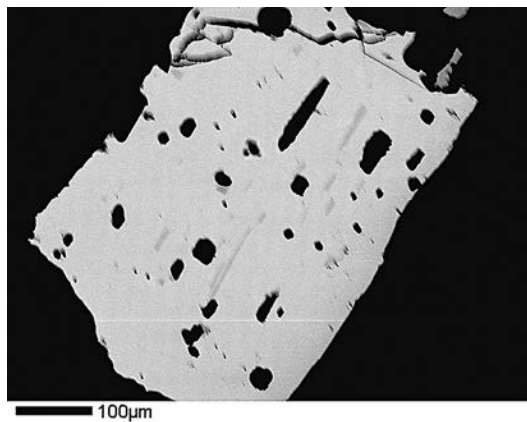


FIG. 8. Backscatter electron image (BEI) showing apparent exsolution lamellae of sylvanite. The darker color of the lamellae is indicative of a lower atomic weight (higher Ag content).

demonstrate that Au and Ag ordering within the krennerite structure may be due to the avoidance of Ag–Te–Ag bonding. The avoidance of this bond restricts the Au to Ag ratio within the structure, giving an observed ratio of approximately 3:1. If this ratio is required to stabilize the krennerite structure, which we believe to be true, then the compositional range of krennerite is limited to being between that of calaverite and sylvanite.

A compositional restriction in krennerite might then explain several of the observations made during the paragenetic portion of this study. Most importantly, it provides evidence that exsolution between krennerite and sylvanite may be possible, as compositional restriction upon cooling is required for exsolution to occur.

ACKNOWLEDGMENTS

The authors wish to thank Dr. Louis J. Cabri for his invaluable contributions while preparing this manuscript, and for allowing reproduction and modification of his original work. We also thank Drs. Bruce A. Geller, Murray W. Hitzman, and Thomas Monecke for their suggestions on improvements to this manuscript. Additional gratitude is extended to Ed Raines and Dr. William W. Atkinson, Jr. for sharing their insight on epithermal telluride mineralization. The X-ray diffraction study was supported by US National Science Foundation Grants EAR0765111 and EAR11-13369 to JRS.

REFERENCES

- CABRI, L.J. (1965) Phase relations in the Au–Ag–Te system and their mineralogical significance. *Journal of Economic Geology* **60**, 1569–1606
- FLACK, H.D. (1983) On enantiomorph-polarity estimation. *Acta Crystallographica* **A39**, 876–881
- GELLER, B.A. (1993) Mineralogy and origin of telluride deposits in Boulder County, Colorado, 731 p. Ph.D. thesis, University of Colorado, Boulder.
- LOVERING, T.S. & GODDARD, E.N. (1950) Geology and Ore Deposits of the Front Range, Colorado. *U.S. Geological Survey Professional Paper* **223**, 289–312
- PERTLIK, F. (1984a) Kristallchemie natürlicher Telluride I. Verfeinerung der Kristallstruktur des Sylvanits; AuAgTe₄. *Tschermaks Mineralogische und Petrographische Mitteilungen* **33**, 203–212
- PERTLIK, F. (1984b) Crystal chemistry of natural tellurides II: Redetermination of the crystal structure of krennerite. *Tschermaks Mineralogische und Petrographische Mitteilungen* **33**, 253–262
- SAUNDERS, J.A. (1986) Petrology, Mineralogy, and Geochemistry of Representative Gold Telluride Ores from Colorado. 171p. Ph.D. thesis, Colorado School of Mines.
- SCHUTTE, W.J. & DEBOER, J.L. (1988) Valence fluctuations in the incommensurately modulated structure of calaverite, AuTe₂. *Acta Crystallographica* **B44**, 486–494
- SHELDRIK, G.M. (1997) SHELXL-97, Program for Refinement of Crystal Structures. University of Göttingen, Germany.
- TUNELL, G. & KSANDA, C.J. (1936) The crystal structure of krennerite. *Washington Academy of Sciences* **26**, 507–509.
- TUNELL, G. & MURATA, K.J. (1950) The atomic arrangement and chemical composition of krennerite. *American Mineralogist* **35**, 959–984.

Received April 22, 2011, revised manuscript accepted January 30, 2012.